Construction and Building Materials 445 (2024) 137939

Contents lists available at ScienceDirect

Construction and Building Materials

journal homepage: www.elsevier.com/locate/conbuildmat

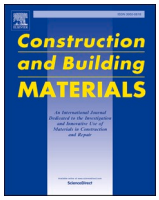

One-year results of the first road surface with the addition of sunflower oil porous capsules

M. Abedraba-Abdalla [a,*], A. Garcia-Hernández [b], F. Haughey [c], Nick Thom [a], Lingling Li [a]

[a] Nottingham Transportation Engineering Centre, Department of Civil Engineering, University of Nottingham, Nottingham NG7 2RD, United Kingdom
[b] Lehrstuhl und Institut für Straßenwesen, Aachen University, Aachen 52074, Germany
[c] Tarmac Trading Ltd, Station Approach, Harlow, Essex CM20 2EL, United Kingdom

ARTICLE INFO

Keywords:
Asphalt surface road
Oil-filled porous capsules
Self-healing
Porous structure asphalt ravelling
Aggregate loss
Road macrotexture
Rutting
Fatigue life

ABSTRACT

This paper presents findings from the first surface course in the UK employing sunflower oil-filled porous capsules as a self-healing additive. The capsules, designed to mitigate ravelling, were tested on a road constructed at an asphalt plant and subjected to a year of traffic in temperatures ranging from below 0°C to 35°C. Spherical in shape with a diameter of about 1.5 mm, the capsules possess a porous structure filled with sunflower oil. Each tonne of asphalt contained 5 kgs of capsules. The material used was Stone Mastic Asphalt (SMA), one of the UK's most utilised surface course materials. Eight sections were built, with four varying binder contents (6.4 %, 5.9 %, 5.5 % and 5.2 %), each with and without capsules. The road performance was evaluated by measuring two indicators: rut depth and surface macrotexture. Results show that the capsules delay fretting progression in wearing courses. Fretting could have resulted from the complex interaction between early life wearing and asphalt compaction by traffic that caused the mastic to move to the road surface. In addition, no considerable difference in rutting was observed between the different materials. Moreover, core samples were extracted from the road before and after traffic and age exposure for further laboratory analysis to assess the long-term performance. Results showed that stone loss resistance in asphalt-containing capsules was 30.02 % lower before ageing and 25.92 % lower after ageing. Furthermore, the stiffness ageing factor was 15–20 % lower in materials with capsules, while the fatigue life remained consistent across all materials.

1. Introduction

Asphalt is commonly used as a pavement surface material for highways and airport runways due to its cost efficiency, comfort, and noise reduction advantages. However, asphalt distress, including ravelling, cracking, and rutting, can impair vehicle movement, compromise safety, and require costly maintenance. Open-graded courses, including Stone Mastic Asphalt (SMA), are designed and installed in high-stress pavement roads due to their strong and stable stone-to-stone skeleton, which gives higher rutting resistance to the mixture and enhances its durability. Despite this, SMA mixtures are susceptible to premature deterioration due to high concentrations of mechanical stress on the road, combined with the ageing of the binder caused by adverse weathering, which leads to ravelling and cracking [1,2,3].

SMA distress has been treated in many ways to improve binder stability and enhance the mixture's compressive strength. For instance, to delay cracking, bitumen has been modified with steel fibres that add high tensile strength and reinforce the matrix within the asphalt [4,5]. Nevertheless, the high cost and the difficulties in handling and mixing the steel fibres constitute a challenge to its practical use [6]. Another alternative to delay the generation of cracks is to enhance the elasticity of the asphalt by adding crumb rubber [7,8], which improves fracture toughness due to the ability of the rubber to maintain elasticity at low temperatures; yet this type of additive has its own sets of challenges, including the instability of the rubber when stored at lower temperatures, the poor compatibility of the polymer and the bitumen, and the increased costs and environmental concerns associated with its use [8,9]. A novel alternative proposes using waste tyres as precursors for asphalt rejuvenators through pyrolysis and distillation processes. This method has shown promising results in restoring the chemical compounds of aged asphalt. However, further research is needed to study the self-healing properties of bitumen.

Self-healing techniques have also been explored to enhance SMA durability against fatigue [10,11,12,13] and ravelling [14,15] through

* Corresponding author.
E-mail address: mariam.abedrabaabdalla@nottingham.ac.uk (M. Abedraba-Abdalla).

https://doi.org/10.1016/j.conbuildmat.2024.137939
Received 2 June 2024; Received in revised form 31 July 2024; Accepted 14 August 2024
Available online 16 August 2024

restoring asphalt chemical compounds in aged materials, which enhances adhesion properties. However, most self-healing technologies lack full-scale road testing and relevant use specifications [16]. Amongst the techniques, encapsulated rejuvenators filled with sunflower oil have shown promising results compared to unmodified asphalt, especially when considering resting periods. This is attributed to the capsules potentially aiding the mastic in recovering some of its strength through its deformability and release of oil, which softens the mastic, enabling it to flow and close microcracks [17,18]. These capsules have been proven to withstand high temperatures, distribute uniformly in the mix, survive after compaction, and not compromise asphalt mechanical properties [13]. Moreover, not only have they been considered as oil-releasing inclusions that reduce mixture viscosity, but recent studies evaluating the stone loss resistance of asphalt under impact loading using the Cantabro machine [14,19] have noted how encapsulated rejuvenators or "porous capsules" cause changes in the aggregate skeleton due to the capsules' inherent energy absorption properties, a function of their internal cellular structure comprising closed foam-like cavities. The cell walls collapse under loading and convert some of the energy into potential energy stored within the deformed structure of the particle [20]. This theory was developed as the testing time during the Cantabro test was insufficient for the rejuvenator to diffuse and promote asphalt self-healing, and hence, the mitigation of ravelling was attributed to cellular capsules' ability to deform absorbing energy gradually.

Furthermore, [19] examined the cellular effect of using 3D-printed lattice structures to substitute oil-filled porous capsules. A fundamental study was performed by subjecting a composite granular medium comprising single-size aggregates to cyclic and monotonic stress. The results confirmed that the cellular structure impacts the aggregate skeleton by increasing aggregate strain after loading, which led to a 24 % increase in energy absorption. Hence, to maximise the efficiency of energy absorption, it has been suggested that porous capsules should constitute part of the aggregate skeleton [21].

To date, including porous particles in asphalt has shown promising and non-negligible effects on asphalt performance based on laboratory testing. However, capsules had yet to be tested on a full-scale field section to determine their ability to withstand mixing and compaction, evaluate the impact of the oil contained on the road's skidding resistance and rutting, evaluate the condition of the capsules in the asphalt following a year of road use, and for future studies to address uncertainties including manufacturing cost and environmental impact, which commonly pose a challenge to the addition of polymeric additives [8]. Hence, this article presents the first long-term results of an experimental road containing polymeric porous capsules filled with oil subjected to traffic, which offers a unique opportunity for long-term performance insights, addressing the current understanding gap with regard to its real-world applicability and performance. The manufacturing of capsules required upscaling of the existing method [13,22,23,24,25,26,27] with a new design and equipment to produce larger quantities. The road was constructed at the Harper Lane asphalt plant in November 2021. It consisted of 8 sections with 4 different binder contents, each with and without capsules. Following the construction, the skid resistance was measured, and periodical visits were conducted to test the road performance by evaluating rut depth and changes in macrotexture. Moreover, further analysis for in-depth insight was conducted in the laboratory using cores obtained from the site. Both site and laboratory data can support the development of theories around the different mechanisms of action of the sunflower oil-filled capsules when added to asphalt.

2. Research methods

2.1. Testing programme

This study is divided into 3 sections that are defined by their aims and methods, which is summarised in Fig. 1 and described below:

a) Porous capsule production: To increase production for the road trial and assess the feasibility of implementing a system capable of producing capsules for larger-scale trials, the manufacturing process was scaled up. Capsules were then analysed to ensure their size and internal features matched those optimised in small-scale production.
b) In-situ data collection: To evaluate the effect of capsules on asphalt performance with varying binder contents, rut depth and surface macrotexture were measured from each section to provide insight into the evolution of the surface behaviour during 1 year of traffic.
c) Laboratory assessment: To evaluate the effect of ageing on asphalt with capsules, cores from outside the wheel paths before and after 2 years of field ageing were extracted and evaluated for changes in volume, stiffness, particle loss, and fatigue resistance.

3. Research materials

3.1. Experimental surface courses

Experimental surface courses were constructed at the Tarmac Harper Lane asphalt plant, located in a limestone quarry in the southern region of England. The location was selected because it was subjected to the heavy traffic of fully laden vehicles, with loads ranging between 32 and 44 tons, and approximately 700 Equivalent Standard Axle Loads (ESALs) per day. To examine the influence of bitumen content on the performance of asphalt, a total of 8 pavement sections were built. These sections consisted of four different asphalt mixtures with varying binder contents of 5.2 %, 5.5 %, 5.9 %, and 6.4 %. Each mixture was divided into two sections, one without capsules and one containing capsule. Fig. 2 shows a schematic layout of the sections with corresponding labels for each. The capsules were manufactured, packed and sealed at the University of Nottingham, and they were delivered to the plant in melting bags of 5 kg each; see Fig. 3 with (a) melting bags containing capsules and (b) an image of loose capsules. The asphalt was mixed at

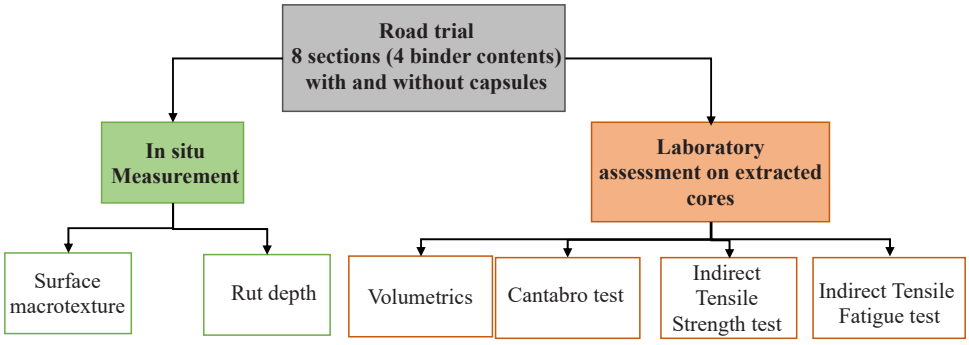

Fig. 1. Graphical experimental plan.

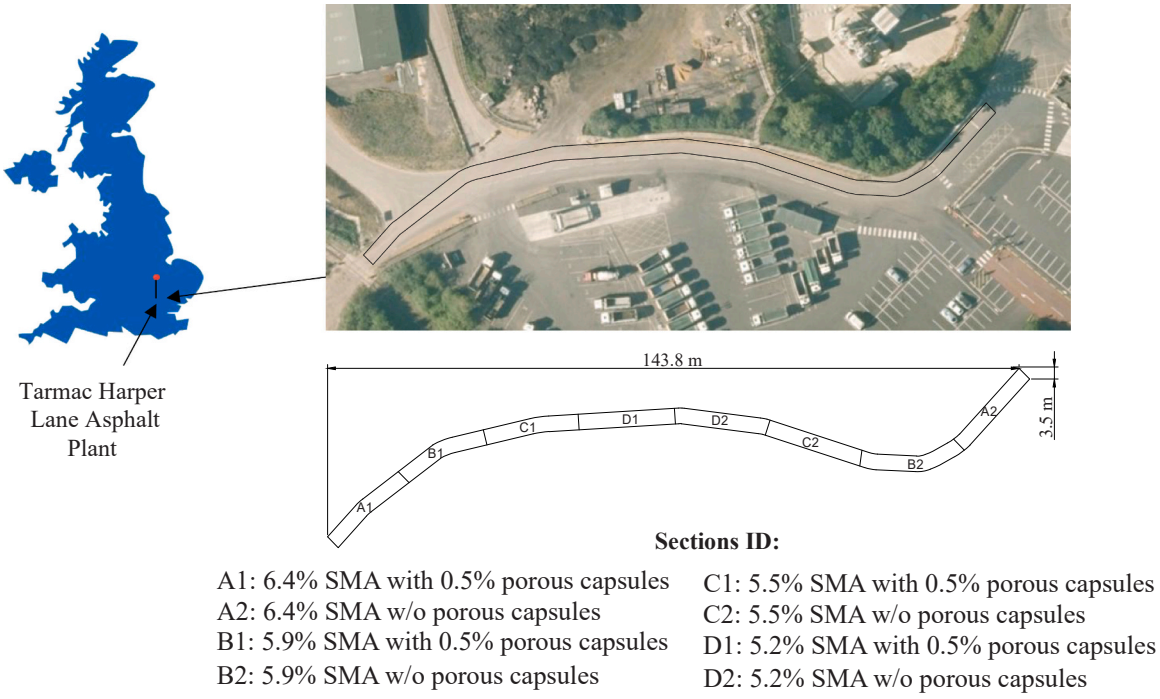

Fig. 2. Road location and schematic representation of the different sections with different mixture types and their labels.

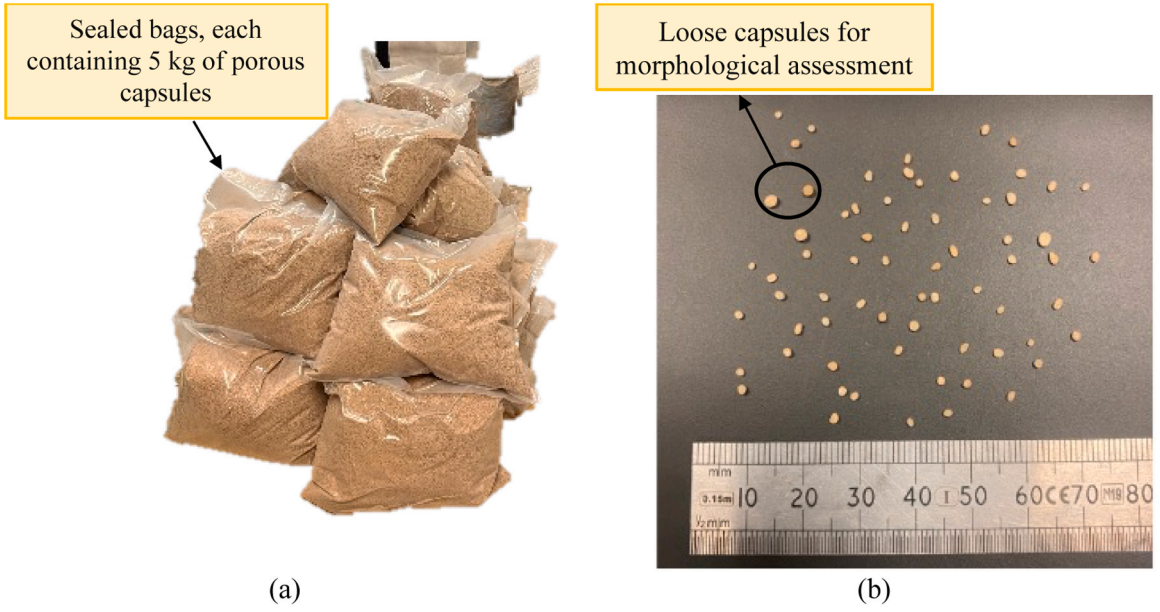

Fig. 3. (a) Sealed bags containing 5 kg of capsules each. (b) Loose individual capsules.

165 ºC for 30 seconds using a drum-facility mix. Previous research has shown that the various mixing stages did not yield any differences in the morphological and mechanical properties of the asphalt. Hence, after mixing the aggregates and bitumen, 0.5 % of capsules by total weight were added as an additive at the end of the mixing phase, second 20 [21].

Each section has a total length of 17.975 m and a width of 3.5 m. The mixtures were laid manually on a 40 mm milled surface, followed by a screed to ensure even distribution and levelling of the asphalt. Lastly, a track paver and a tandem roller were used for compaction at approximately 140 ºC. Images of the texture were taken after the asphalt was laid, as seen in Fig. 4, where the surface courses of test section B with 5.9 % binder content with and without capsules were visually indistinguishable. The sections were exposed to temperatures fluctuating between below 0 ºC and exceeding 30 ºC, and the annual average precipitation in the area amounted to 622 mm. Due to the site's proximity to a limestone quarry, the road surfaces were often covered with dust. Therefore, before taking any performance indicator measurements from the sections, they were subjected to jet-washing to guarantee the elimination of surface debris. During the first year after the road construction, a total of 10 visits were conducted to examine and measure rut depth and macrotexture.

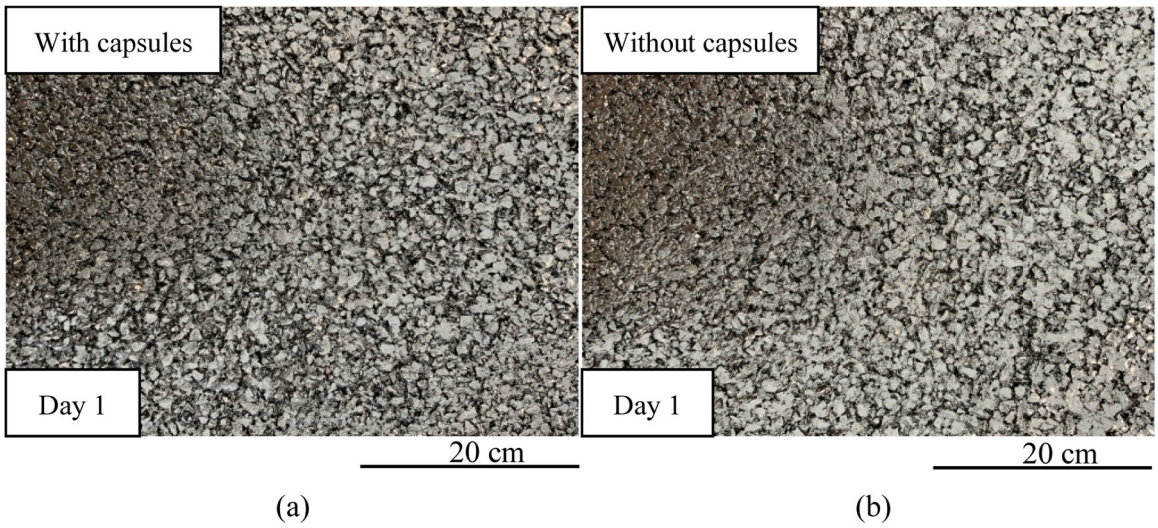

Fig. 4. Images of the test sections. (a) with capsules. (b) without capsules.

3.2. Asphalt materials

Stone Mastic Asphalt, SMA, 10 mm maximum particle size, in accordance with [28], was manufactured with 0 % and 0.5 % capsules [31] by the total weight of the mixture. The components used were gritstone (2.800 g/cm^3), granite dust (2.670 g/cm^3), cellulose fibre (0.095 g/cm^3) and 40/60 pen bitumen (1.027 g/cm^3), and the maximum density of the mixture was 2.455 g/cm^3. The mixture was composed of 15.4 % granite dust, 16 % 6 mm gritstone, 48.4 % 10 mm gritstone, 5 % 14 mm gritstone, 8.5 % filler, 0.3 % fibre and 4 binder contents, 6.4 %, 5.9 %, 5.5 % and 5.2 %. The mixture was designed to have a 4 % air-void content; see the detailed composition in Table 1. Furthermore, 3 cores of 150 mm diameter and 40 mm thickness were extracted per section from the centre line of the road on day 1 after construction and after 2 years of climate exposure. The samples were tested in the laboratory to evaluate the effect of ageing on its mechanical performance.

3.3. Capsules manufacturing and characterisation

This study required around 150 kg of porous particles to construct the road trial. The porous capsules (bulk density: 1.116 g/cm^3 [15]) were composed of sodium alginate, sunflower oil, and water. The cellular structure of the cross-linked calcium-alginate polymer capsules was formed through the external ionic gelation of sodium alginate ($C_6H_7O_6Na$) in the presence of calcium chloride ($CaCl_2$), both supplied by Sigma Aldrich with bulk densities of 0.7 g/cm^3 and 2.1 g/cm^3, respectively [29]. The cavities of the polymer structure contained commercial sunflower oil (bulk density: 0.92 g/cm^3), a bitumen-compatible additive used as a rejuvenator. A detailed description of the porous capsules' composition and mechanical properties can be found in previous research [13,22,23,24,25,26,27].

Table 1
Asphalt's composition with and without capsules.

Aggregate size	Mass %	Mass (kg/section) with capsules	Mass (kg/section) with capsules
14	5.00	309.0	309.0
10	48.40	2990.0	2990.0
6	16.00	988.0	988.0
Dust	15.40	951.0	951.0
Filler	8.50	525.0	525.0
Fibre	0.30	19.0	19.0
Bitumen 40/60	6.4; 5.9; 5.5; 5.2	395;365;340;321	395;365;340;321
Capsules	0.50	0.0	31.0

The manufacturing of capsules for this study required upscaling of the existing method [24,25,26,27]. Fig. 5 shows an image of the upgraded manufacturing system at the University of Nottingham. The oil/water and oil/alginate mass ratios used for each mix are 4/25 and 15/25, respectively. The manufacturing process at a larger scale includes the following stages, which are depicted in Fig. 5: i) Emulsification of water, calcium chloride, and oil emulsion in a high-speed disperser (A) at 1125 rpm for 10 minutes, ii) Emulsion transfer into a deposit tank (B), which is connected to a water pump (C); iii) Preparation of a calcium chloride solution with 2 % water in a pump tank collector (D), stirring using a wave maker. The emulsion then flows at a rate of 60 l per minute down the PVC tube to the stainless-steel pipes (E) and streams through the 3D-printing nozzles of 1 mm diameter; iv) The spherical capsules form inside the chloride solution by adjusting the flow using ball valves until the liquid narrows as it descends. This adjustment increases the pressure within the stream and causes the stream of the emulsion to become narrower. This stream narrowing leads to the formation of drops as the liquid separates into discrete volumes [30] due to the combination of surface tension forces, gravitational effects and external perturbations; v) The capsules are collected, rinsed and coated with filler; vi) The last step is to dry the capsules in a food dehydrator at 50ºC for 24 hours, seal them in polythene bags and store them in a cool area to avoid oxidation of the sunflower oil.

3.4. Imaging acquisition and analysis

The internal and external structure of porous particles were characterised using a FEI Quanta 650 Environmental Scanning Electron Microscope (ESEM), operated in wet mode [31] due to the presence of oil in the cavities of the porous capsule. Surface pre-treatment was unnecessary due to the combination of high gas pressure and sample cooling, which allowed for precise control of the thermodynamic stability of wet specimens, in contrast to SEM [32]. Several particles were cut using a carbon steel flat scalpel blade to create smooth and clean cross-sectional areas. These particles were placed on double-sided tape and inserted into a loading channel. The tests were conducted with a field emission electron gun in environmental mode at 25°C. The ESEM operated at 15 kV, and 20 kV accelerating voltage and the magnification was set to 500x and 1000x. The images obtained were post-processed using ImageJ.

Additional analysis on the morphology and spatial distribution of the capsules embedded within the in-situ asphalt was performed using a CT

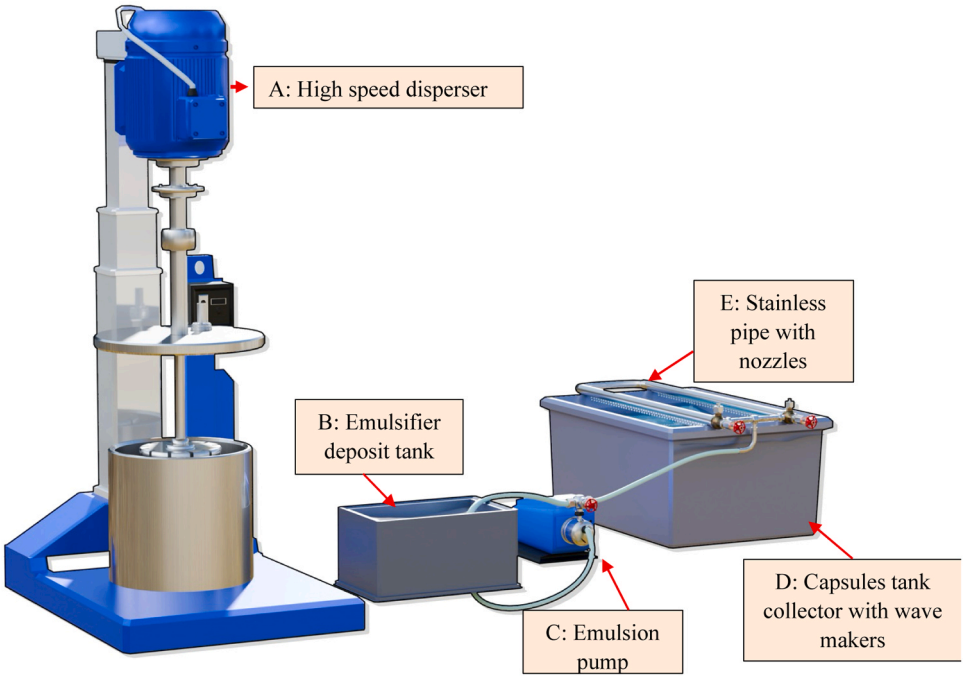

Fig. 5. Porous capsules' manufacturing system at the University of Nottingham.

scanning device, Phoenix Vtomex M, operating at 300 kV and 100 μm of spatial resolution on cores extracted post-road construction and after a year of the road trial. The test was conducted on cores measuring 5 mm in diameter and 40 mm, and the images obtained were reconstructed using VGStudio MAX software (2023.1).

3.5. On-site measurement: skidding resistance, rutting and macrotexture

The release of oil from the capsules into the mixture could affect the skid resistance of the asphalt, particularly during the post-construction phase when the aggregates retain a layer of bitumen. The friction depends on the macrotexture and type of aggregate in the surface course after the film on the surface of the aggregates has been removed [33]. Hence, the British Pendulum Test was conducted on all sections after construction following BS EN 13036–4 [34]. The device measures low-speed friction to assess the microstructure of the pavement surface by moving a rubber slider attached at the end of the pendulum. The frictional force diminishes the pendulum's kinetic energy as the slider moves. The reduction in kinetic energy and the magnitude of the frictional force in the pavement can be quantified by measuring the change in the pendulum height before and after the slider crosses the pavement. The temperature recorded was 12 ºC, and each section's Pendulum Test Value (PTV) was determined using the average of 3 tests from each section.

In addition, the surface texture was measured through the Mean Profile Depth, a macrotexture descriptor in the wavelength domain between (0.5 and 50 mm), using an Ames laser texture scanner (LTS) 9400, which can precisely measure any surface's texture composition and record the elevation height data of scanned points after filtering them using a 3 mm Butterworth second-order filter. The scanner covers a 101.6 mm long and 76.2 mm wide area, and it was configured to conduct measurements along 10 lines and 250 lines for full 3D reconstruction. The LTS has a dot size of around 0.050 mm when positioned at 42 mm, offers horizontal sampling resolutions of 0.01 mm, and 0.5024 mm distance between two points, which satisfies the macrotexture specification [35]. The data was obtained and analysed following BS EN ISO 13473–1 [36]. A total of 15 MPD measurements were acquired for each asphalt section, with sampling points randomly distributed across the wheel path. Subsequently, the mean of these measurements was determined to represent the asphalt macrotexture. Fig. 6 shows the laser box.

Rut depth, another surface performance indicator, was measured using a 3 m foldable straight edge with 12.5 mm blocks, as shown in Fig. 7, which was placed on the asphalt pavement. The distance from the straight edge to the pavement was recorded with a metric graduated wedge across the section lane. On the trial site, measurements were taken at 5 m intervals.

3.6. Laboratory assessment

The performance of asphalt, both with and without the inclusion of oil-filled porous capsules, subjected to field ageing was further examined through laboratory analysis for changes in volume, stiffness,

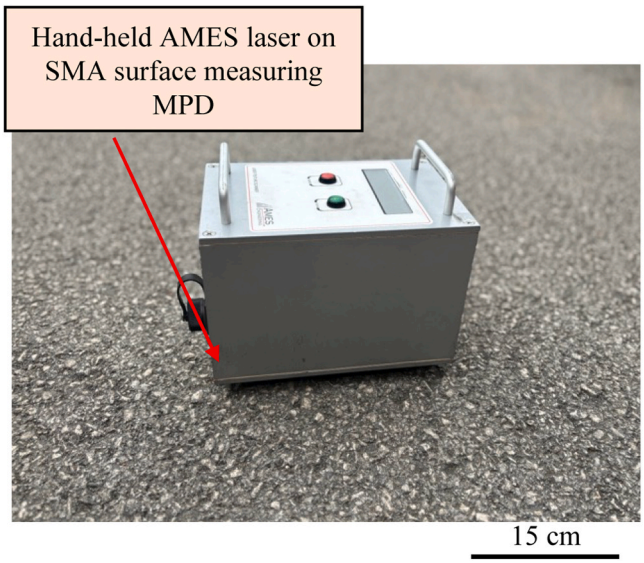

Fig. 6. Ames Laser Texture Scanner 9400.

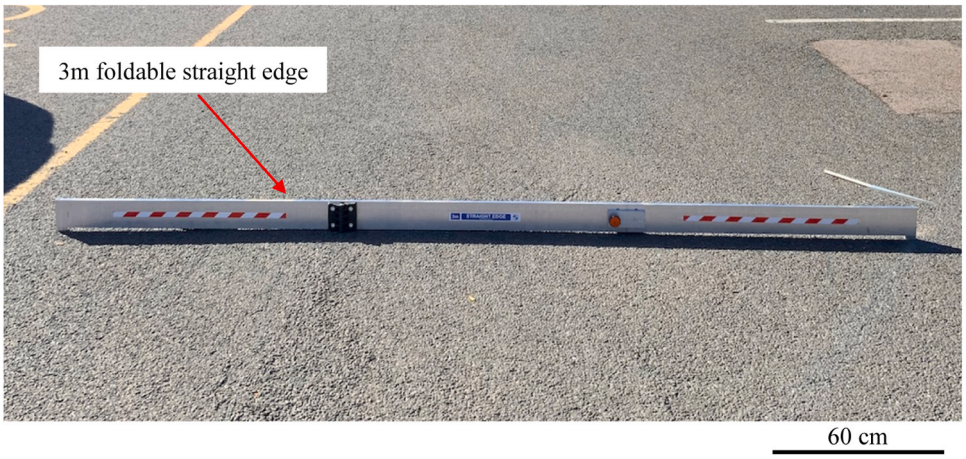

Fig. 7. 3 m foldable straight edge.

abrasion, and fatigue resistance.

3.6.1. Indirect tensile stiffness modulus test

To evaluate the effect of ageing on the mixture with and without porous capsules, the authors employed a simplistic approach using the Indirect Tensile Stiffness Modulus (ITSM), which is correlated to the cracking properties of the pavement [37]. Several researchers have used the resilient modulus to study the effect of ageing on asphalt mixtures. The test was conducted on extracted ones from the road trial immediately after construction and after a year of continuous traffic. The test samples were preconditioned for 4 hours at three different temperatures (10 ºC and 20 ºC). No higher temperatures were used as the same samples needed to remain undamaged since they were to be used for other non-destructive and destructive tests. The horizontal displacement was measured using two oppositely positioned Linear Variable Differential Transformers (LVDTs). The test procedure was repeated across a perpendicular diameter, and the measured stiffness modulus of the test pulses from the two tested diameters was recorded as the stiffness modulus of the specimen following BS EN 12697–26 [38].

3.6.2. Aggregate loss test

Traffic and ageing can impact the capsules' performance as well as mixture adhesion; hence the abrasive resistance of the field mixture after 2 years of climate exposure was studied. The test was conducted in a Los Angeles abrasion machine following the same procedure as in [39].

3.6.3. Indirect tensile fatigue test

To assess the fatigue life of aged and unaged field mixtures, the Indirect Tensile Fatigue test was adopted, as outlined in BS EN 12697–33 (Appendix F) [40]. The equipment used in this study only operates in a stress-controlled mode and it was selected to ensure comparability with previous studies, which employed a similar setup. The equipment used was a Cooper Testing Universal Machine UTM (NU-10). Before the testing, the specimens were conditioned in the UTM chamber at 10 °C for 6 hours. Subsequently, the samples were subjected to a force-controlled haversine loading with 0.1 seconds loading and 0.4 seconds resting periods with a loading frequency of 2 Hz, exerted through the vertical diametral plane of the specimens. The test was carried out in a controlled stress mode, where a single horizontal stress value of 600 kPa was chosen. The stiffness modulus and rate of decay was calculated through Eq. 1. The failure criteria encompassed the total failure of the sample or a 50 % stiffness reduction where applicable [41].

$$S_m = \frac{\sigma_a}{\varepsilon_a} \bullet (1 + 3\nu) \bullet 10^6 \quad (1)$$

Where S_m is the stiffness modulus, ε_a is the maximum intitial tensile strain, σ_a is the maximum horizontal stress and ν is the poission ratio selected as 0.35.

4. Results and discussion

4.1. Structure of porous capsules and mechanical properties

ESEM images revealed a matrix structure composed of connected pores, as shown in Fig. 8. Further processing of the images revealed that the matrix comprised 59.5 % alginate and 40.5 % oil, which is enclosed inside the cavities. The internal structure composition and dimensions are not compromised by the larger components ratio used in this design, and it is similar to the ones discussed in [25,42]. The porous structure is similar to that of cellular materials with polyhedral cell geometry that, under compression, deform via a combination of cell bending and twisting of the individual cells [43].

The manufacturing at a larger scale did not affect the morphology and inner structure of the capsules, as visually, they appear to be similar to those manufactured at a smaller scale in previous studies [14]. By examining the capsules under the uniaxial compression test following [29], the plotted stress and strain showed a curve with 3 distinct regions, defined as an elastic, plateau and densification, which is consistent with the description found on cellular materials behaviour under compressive strength test. See Fig. 9 illustrating a single capsule behaviour under compression test. The plateau region indicates plastic deformation [44]. If the porous capsule behaves similarly to a cellular material or foam, significant energy dissipation should occur in this region, where the walls begin to deform under nearly constant load [45]. This is likely where the maximum release of oil happens, as it should be expelled when the cell walls deform and begin to collapse.

4.2. Effect of field ageing on asphalt volumetric properties, stiffness modulus, particle loss resistance and fatigue life

Volumetric properties, one of the main factors affecting asphalt performance [46], are directly influenced by changes in binder properties resulting from ageing and traffic [47]. Fig. 10 (a) illustrates the average void content of 3 asphalt cores extracted from the lane centre of each road section before and after two years of field ageing. The 40 mm SMA mixture across the 8 different sections exhibited a higher average void content than the target void design. To discern the factors that could affect the fundamental properties of asphalt after compaction, including compaction efficiency, binder grading, and aggregate gradation [48,49,50], three specimens were manufactured in the laboratory from each bulk site material using a Marshall compactor, and assessed. Results showed that the void content was closer to the target void of 4 %,

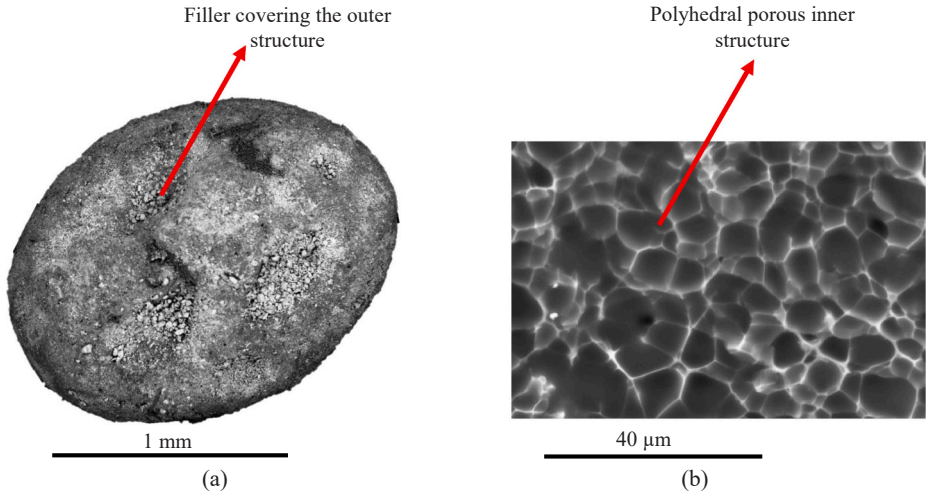

Fig. 8. Images of the capsules. (a) Detail of a capsule. (b) Internal porous structure of the capsule.

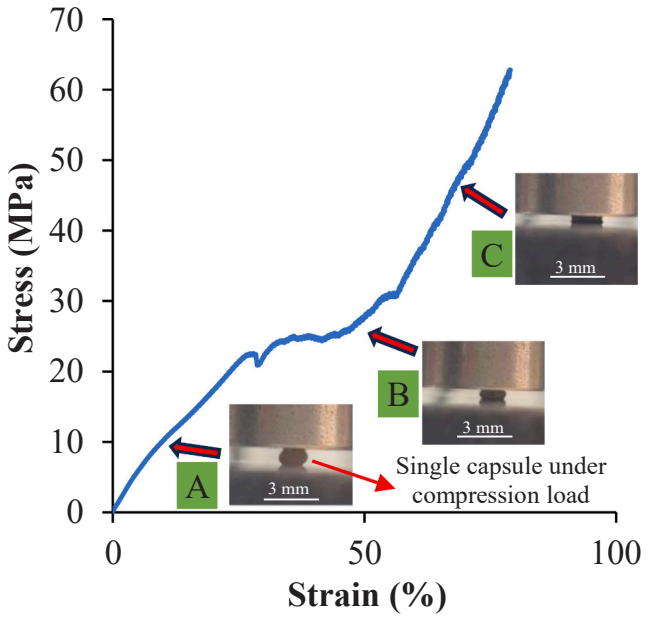

Fig. 9. Different stages during the stress-strain response of a porous capsule under compression testing; A: Elastic region, B: Plateau region, C: Densification.

and there was not much difference between specimens with and without capsules, as seen in Fig. 10 (b), suggesting that the higher AVC observed in the field before traffic could be attributed to compaction efficiency issues. The force applied through compaction, or the selected temperature, might not have been sufficient to overcome the interlocking and friction of the aggregates and compact as densely as intended [48].

Furthermore, asphalt materials A (6.4 %) and B (5.9 %) containing porous capsules exhibited approximately 1 % lower void content compared to those without capsules, whereas C (5.5 %) and D (5.2 %) displayed negligible statistical differences. This reduction in void observed contrasts with the most recent findings [51], suggesting that the addition of 0.5 % of capsules in SMA with 6.4 % binder content did not affect the final void content. The observed difference in void content can be attributed to the fact that road compaction could have led to more deformation of capsules compared to the laboratory compaction methods. The increase of deformed capsules caused more oil release that enhanced the compaction process in materials with higher binder content by allowing the aggregates to roll and slide better due to the increased lubrication action between the aggregates, leading to a different material skeleton and, consequently, a reduction in void content.

On the other hand, volumetric analysis of asphalt after two years of ageing exposure revealed a reduction in void content for both materials across the different sections. The decrease in AVC could be attributed to two main factors: first, the enhanced compaction of the surface layer induced by vehicles, which, despite analysed cores having been extracted from the centre line, may still have received some traffic as the wheel path patterns are not defined; second, the migration of dust and sediments into the internal void structure. The latter phenomenon was observed upon inspecting all fractured cores post-fatigue testing, revealing the accumulation of dust within the voids, as illustrated in Fig. 11. The site's exposure to surface detritus from lorries exporting aggregates increases the presence of dust, and, despite the jet washing that took place prior to the periodic site performance measurements, the inherent susceptibility of porous mixtures to clogging facilitates the accumulation of sediment due to their high void contents [51].

Moreover, Fig. 12 shows the average stiffness modulus value at 10°C and 20°C obtained from each section before and after 2 years of field ageing. At both temperatures, it was observed that all asphalt mixtures with higher binder content, materials A and B, exhibited lower stiffness values compared to those with lower binder content, materials C and D. This aligns with [52] and suggests that binder content in this case may have a more significant influence on stiffness than void content. In addition, the materials with lower binder content have lower binder film thickness surrounding the aggregates, increasing the contact between aggregates, which is expected to contribute to the load-bearing capacity [53] and thus result in higher stiffness material.

Regarding the difference between with and without capsules, cores with capsules in materials A and B showed a similar modulus to those without capsules, consistent with the findings in [54]. However, as seen in Fig. 12, in materials C and D, the ones with lower binder content, the stiffness of asphalt with capsules is 15 %-20 % lower than without capsules. This is likely attributed to the following theory: A different stone-to-stone skeleton configuration is formed when there is lower binder content, which facilitates higher particle contact reinforcement, allowing the capsules to become part of the aggregate skeleton rather than flowing in the mastic, where they experience more deformation, further contributing to the observed difference in modulus. This also supports the theories proposed by [54] and [14] regarding the limitation of the capsule's performance if it does not constitute part of the aggregate skeleton.

On the other hand, after two years of ageing, all four materials, both with and without capsules, exhibited an increase in stiffness. This

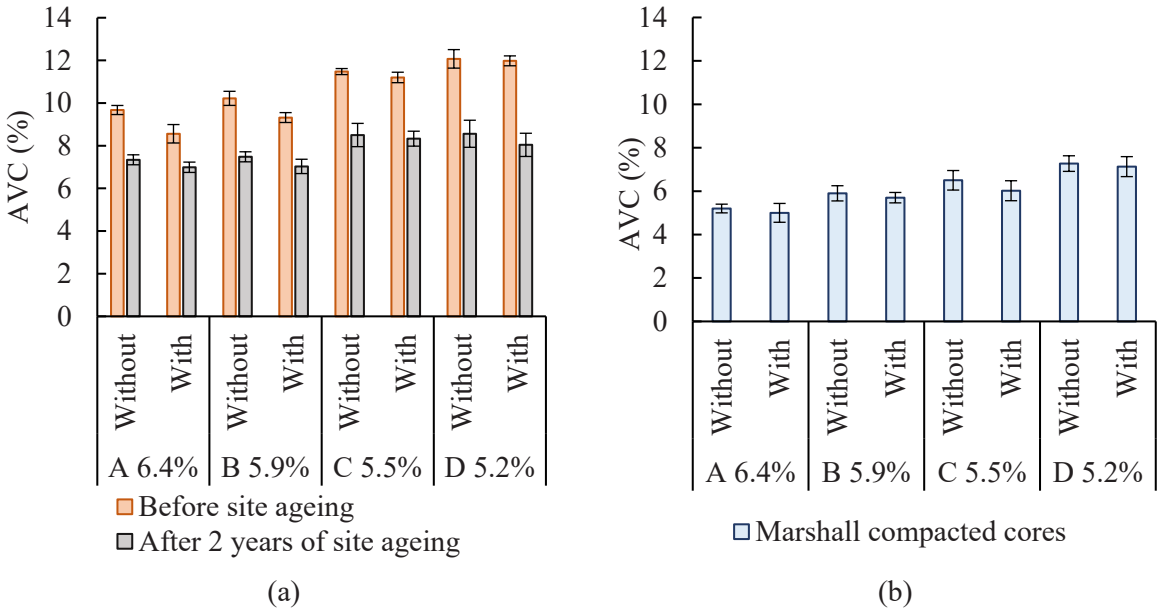

Fig. 10. Air void results. (a) AVC of cores extracted from each section before and after two years of site ageing. (b) AVC of cores manufactured from trial bulk material using Marshall compactor.

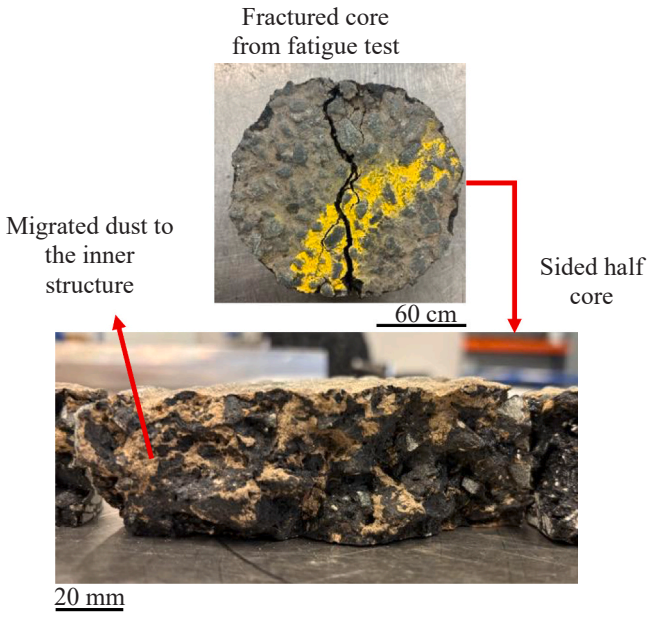

Fig. 11. Fractured fatigue core and inner observation of the material with visible dust accumulation in the inner structure.

increase is attributed to a combination of factors discussed in the above sections, including dust accumulation, densification, changes in void content, and the overall ageing of the material. The resultant ageing factor (E_{aged}/ E_{unaged}) is higher for the lower binder content cores. This is because the lower the binder content in the mixture, the greater the void content, which in turn increases the exposure of the material to oxygen and temperature. This exposure accelerates the hardening process of the material [55,56]

Furthermore, the stiffness modulus of cores A and B, with porous capsules and after 2 years of ageing, is statistically lower than that of the controlled material at both temperatures. This observation could be attributed to several proposed explanations: i) The release of oil from the capsules might soften the binder [60], delaying it from ageing by recovering part of its original stiffness [54]. ii) The deformation of the capsules might absorb energy [18] from traffic, which could otherwise distribute to the mastic and accelerate ageing. iii) This deformation of the capsules might also redistribute the loads by increasing contacts between the aggregates, as the aggregates have been found to carry more than 75 % of the compressive load [57], and effectively transmit it to all points within the structure to reduce the failed contacts by improving the contact mechanical behaviour. The validation of these proposed theories and the study of the load transfer mechanism of asphalt mixture with porous capsules requires further investigation through DEM [58] Understanding asphalt stiffness evolution can provide insight into the ageing and densification process of the material, not only the damage.

What is more, Fig. 13 (a) and (b) show the results of mass loss following the Cantabro test conducted on asphalt cores both before and after 2 years of ageing. The test indirectly indicates the cohesion and adhesion resistance of the mixture [59]. From the results, it is notable that all cores before ageing, irrespective of whether they contain capsules or not, exhibited lower accumulated mass loss, compared to cores subjected to ageing and subsequent densification. The ageing of the material from the combination of different environmental, mechanical, and other phenomena that inevitably occurred during the service of the pavement, have degraded the aromatics and resins in the binder, which affected the adhesion of the asphalt binder and aggregate interface [60], limiting the aggregate-binder adhesion force [61] and thus affecting the total adhesion strength of the asphalt mixture [62], resulting in increased aggregate dislodgment during the Cantabro test. In addition, the clogged sediments that were pushed by the traffic into the voids, as seen in Fig. 11, might have also affected the adhesiveness of the mastic by trapping moisture that facilitated oxidative ageing.

Upon examining the results of abrasion resistance for the specimens containing capsules, it is evident from Fig. 13 that samples containing capsules showed lower mass loss compared to those without, both before and after ageing. This observation aligns with previous studies [21], [63] assessing asphalt abrasive resistance only between the mixtures with 6.4 % binder content. Additionally, it is also observed that the difference in mass loss between specimens with and without capsules reduces as binder content decreases. However, the abrasive resistance after exposure to traffic is evaluated for the first time in this study, and it continues to show a decrease in aggregate loss, which is only possible

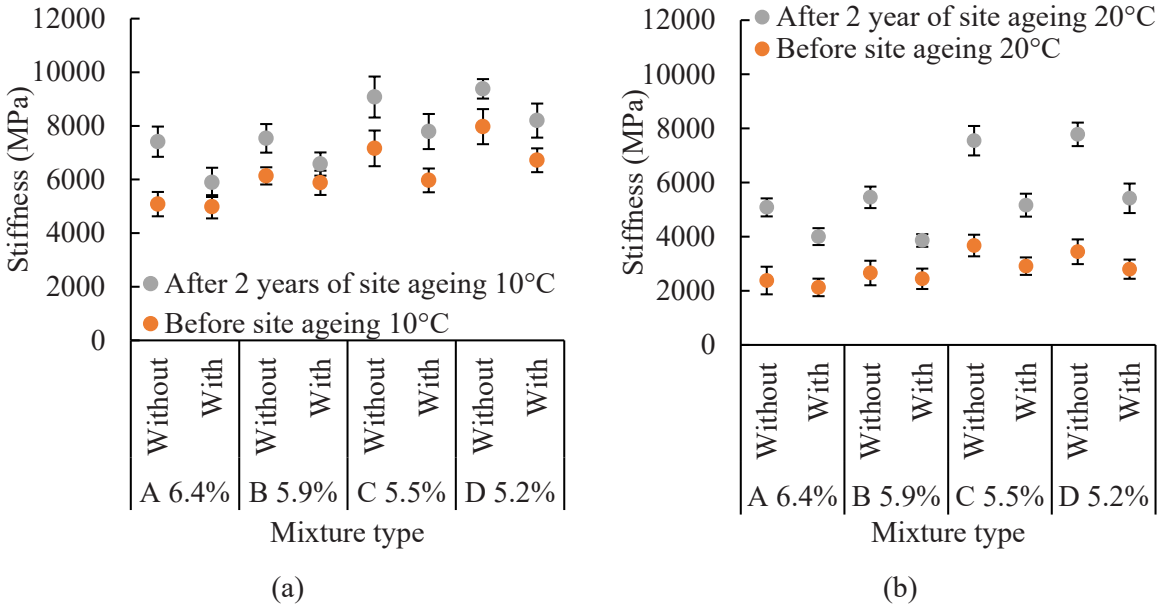

Fig. 12. Stiffness measurement at 10° and 20°. (a) Measured stiffness on cores extracted from the road section before and after site ageing at 10 °C. (b) Measured stiffness on cores extracted from the road section before and after site ageing at 20 °C.

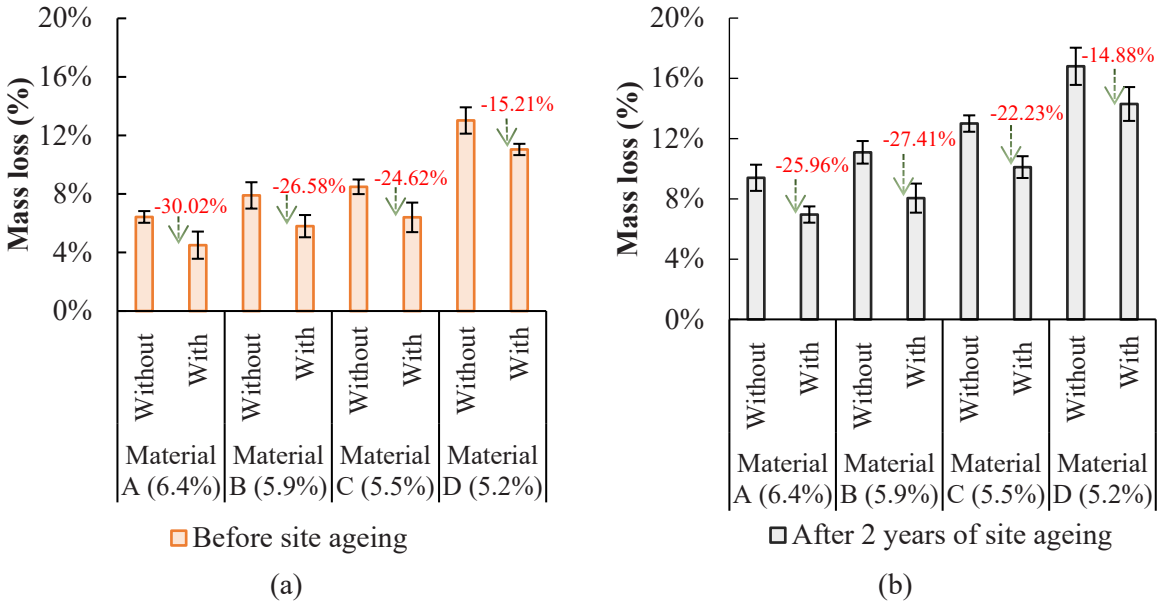

Fig. 13. Particle loss results from the Cantabro test. (a) Before ageing (b) after 2 years of ageing.

because the capsules are still effective in the asphalt. Fig. 14 shows a constructed CT scan of extracted cores after ageing, showing the presence of porous capsules that have contributed to the observed decrease in mass loss.

After evaluation of the stiffness modulus and abrasion resistance, the fatigue service life of asphalt with and without capsules was analysed. Due to the limited availability of the extracted cores from the site, only one core per material was subjected to cyclic load under a constant stress amplitude of 600 kPa. Previous studies conducted on the same set-up and materials [11] showed either similar fatigue behaviour [54] or a 15 % lower life compared to those without capsules [11]. Fig. 15 shows the evolution of the stiffness (E) with loading cycles of the different specimens with varying binder content. The stiffness decay was normalised to the values at the 100th load application (E_{100}), according to [64]. The selected failure criterion after reviewing the results was the total number of cycles achieved at the end of the test, rather than the usual 50 % reduction of stiffness criterion, as some of the materials failed before reaching 50 % of their initial stiffness. The analysis revealed that mixtures from the unaged cores exhibited slower stiffness decay than the aged ones, possibly because the ageing impact on the mechanical structure of binders decreased the adhesion between aggregates and mastic [65], and thus created a stiffer and more embrittled mixture susceptible to faster cracks growth and propagation [55].

In addition, materials A and B, unaged and aged, lasted twice as long as materials C and D. Also, as commonly found, a higher binder content gives a higher fatigue life, as there is more mastic for the crack to grow through [66]. Moreover, upon analysing each material, there is very little difference between asphalt material A and B with and without capsules, perhaps slightly shortened life with capsules, consistent with [11]. Meanwhile, for cores with capsules and lower binder content, C

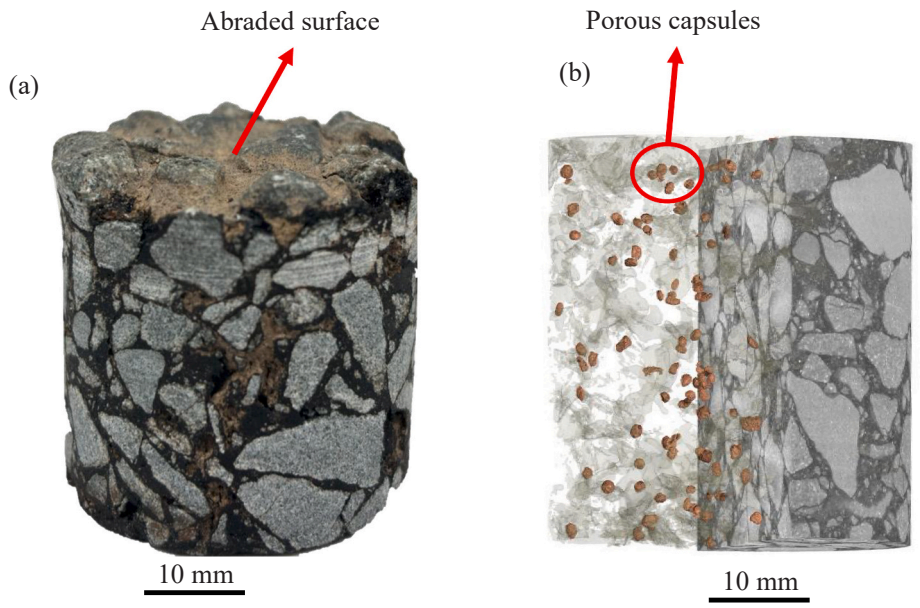

Fig. 14. (a) Extracted core from the quarry after 2 years of service, showing its abraded surface (b) Constructed CT-scan of extracted cores showing porous capsules present and alive.

and D, the decay rate ratio was similar, maybe better for aged materials with capsules. This finding could support the theory that the capsule's performance is enhanced with lower binder content, as they become part of the aggregate skeleton, hence distributing the load better. The results from the fatigue test require further investigation into the effect of different frequencies, temperatures, and loading amplitudes on the fatigue life of asphalt-containing porous capsules when integrated into the aggregate skeleton.

4.3. On-site results: Skidding resistance, rutting and macrotexture

Macrotexture evolution, rut depth and skidding resistance data are plotted in Table 2, Fig. 16 and Fig. 17, respectively, as asphalt surface performance indicators to evaluate the effect of the porous capsules on the evolution of SMA surface performance. Table 2 shows the skid resistance of the asphalt pavement in its so-called "early life" [67] after construction before the scouring of the initial film located on the surface. The pendulum test was conducted on all 8 sections with and without capsules, with the average PTV results from three measurements presented in Table 2. The results indicate that the materials with capsules generally exhibit lower average friction than those without capsules, although both fall within the same category classification of good skid resistance according to ASTM E303–22 [68]. Only the 5.2 % binder content material presented the same PTV average for materials with and without porous capsules. The reduction of PTV value observed in materials A, B, and C with capsules is possibly due to the release of some oil during compaction, which mixed with the binder and acted as a coating interface between the aggregates and the wheels, decreasing the friction.

Fig. 16 depicts the texture evolution of the four materials with varying binder content, (a) without capsules and (b) with capsules. Fig. 17 shows the evolution of rutting with time. The MPD curve reveals a three-stage evolution for all materials. The first stage is characterised by a decay in macrotexture, which peaks at 60 days, possibly caused by the migration of the bitumen from further compaction and the occlusion of voids as dust from trucks accumulates. Despite starting with similar MPD values in the range of 0.83–1.2 mm, those without capsules reach the highest upper limit of the range, and those with capsules have the lowest end value. This discrepancy can be attributed to the higher air void content post-compaction for asphalt without capsules in materials A and B. The decay slope in the first stage is steeper for materials without capsules, registering a lower MPD value at day 60 than with capsules. Coincidentally, the average rutting also decreases for both materials. In addition, Fig. 18 shows a 3D reconstructed image extracted from 250 scanned lines with the laser on day 1 and after 60 days in the same area of section A, which revealed a change in texture over time. The scans from day 60 show less texture, with aggregates covered by more mastic and fewer voids on the surface. This observation could possibly support the theory of bitumen migration to the surface.

After 60 days, both macrotexture and rutting increased and entered the second stage, where wearing the migrated bitumen occurs as a combination of the continuous passing of wheels and the abrasive effect of dust on the road mastic. One can imagine that after compaction, aggregates are fully packed and macrotexture is low, and after the initial wearing, the abrasion rate enters the third stage, where it is constant until the macrotexture is higher than the dust size where light severity [69] ravelling begins. As shown in the schematic of MPD evolution in Fig. 19, which presents a prediction based on the observed macrotexture results, the macrotexture at any point in the pavement's life results from the complex interaction between wear and compaction. Wear increases continuously, while compaction decreases until it stabilises. The first stage of this process is migration, followed by mastic wear, then macrotexture stability, and finally, the stage where stripping may start to occur.

The macrotexture data and rutting evolution after 60 days to 360 days, along with the mechanical response from the laboratory assessment, might aid in evaluating the theories devolved around the mechanism of porous capsules. However, additional data from site measurement is needed to support the theory of the porous capsules in delaying asphalt stripping by providing the matrix with enhanced load transferring nodes across the skeleton through the deformations of the capsules, where absorbing of energy takes place, allowing the migration of binder to be slower and the aggregates to have a cushioning effect, therefore delaying the first aggregate dislodgment caused. Lastly, the final aim is to use the evolution trends and other experimental measurements to predict the progression of surface performance through mathematical models.

5. Conclusions

The inclusion of oil-filled porous capsules has shown its potential to

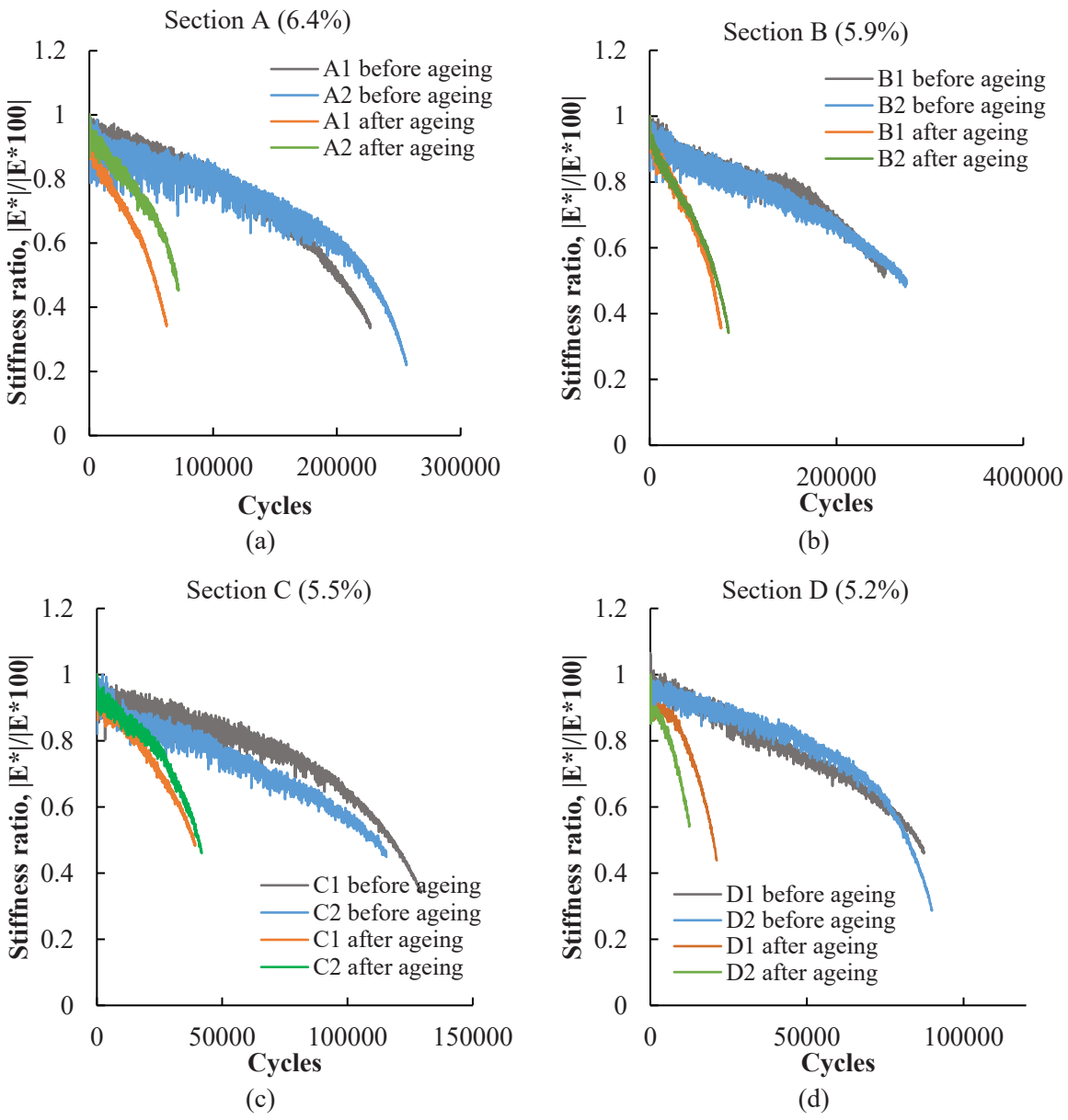

Fig. 15. Stiffness ratio decay vs cycles. (a) Stiffness decay section A (6.4 %), with (A1) and without capsules (A2); (b) Stiffness decay for section B (5.9 %) with (B1) and without capsules (B2); (c) Stiffness decay for section C (5.5 %) with (C1) and without capsules (C2); (d) Stiffness decay for section D (5.2 %) with (D1) and without capsules (D2).

Table 2
Average Pendulum Test value obtained from three measured points for each section.

Road/Location	Average corrected PTV
A1: 6.4 % SMA with capsules	61 ± 2.21
A2: 6.4 % SMA w/o capsules	78 ± 1.76
B1: 5.9 % SMA with capsules	67 ± 2.49
B2: 5.9 % SMA w/o capsules	75 ± 3.34
C1: 5.4 % SMA with capsules	69 ± 6.17
C2: 5.4 % SMA w/o capsules	79 ± 1.60
D1: 5.2 % SMA with capsules	69 ± 2.56
D2: 5.2 % SMA w/o capsules	69 ± 1.74

improve pavement durability through laboratory testing. However, its practical use and long-term performance require additional real-world testing to assess its effectiveness fully. This study offers a unique opportunity for long-term performance insight for asphalt with porous capsules, addressing the current understanding gap of its real-world applicability and performance. An upscaling of the capsule manufacturing equipment was developed, enabling an increase in the production rate and the construction of a trial road site. The constructed road has a length of 148 m, and the selected section of the pavement is divided into 2 main segments: a section with capsules and one without. Road performance indicators were periodically measured on-site. Extracted cores before and after 2 years of ageing were studied in the laboratory to assess their mechanical performance. The main findings can be summarised as follows for materials:

1. Asphalt with porous capsules compacted on site showed a 1 % lower void content than the reference mixture. The deformation of the capsule and subsequent release of oil suggests increased lubrication between the matrix components, allowing the aggregates to roll and slide better, leading to a distinct aggregate skeleton. Following

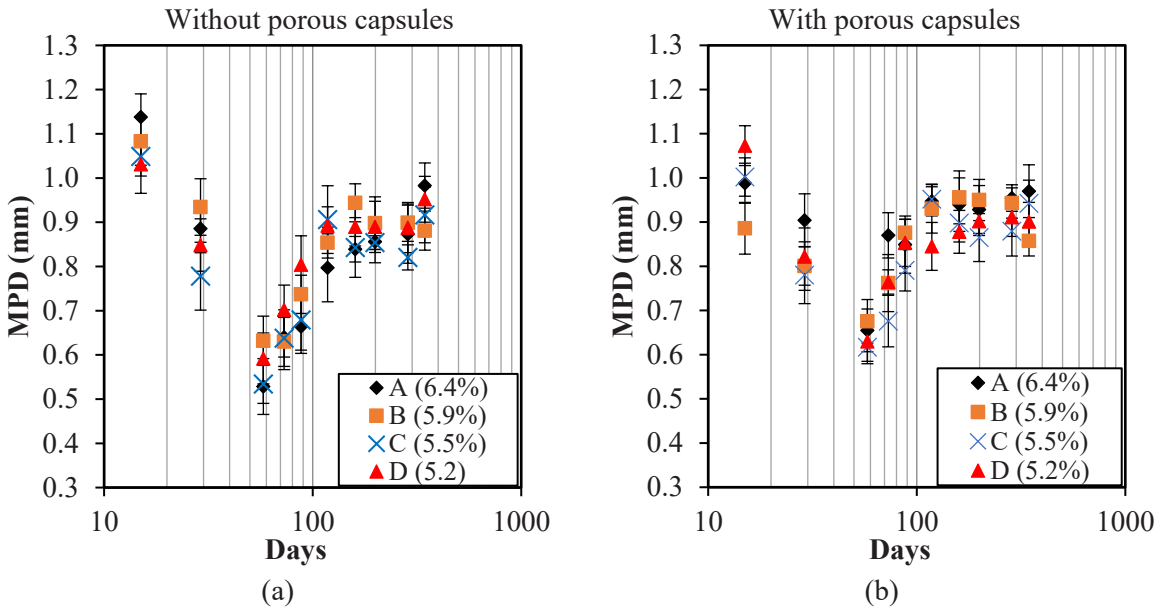

Fig. 16. MPD evolution for each section with and without capsules.

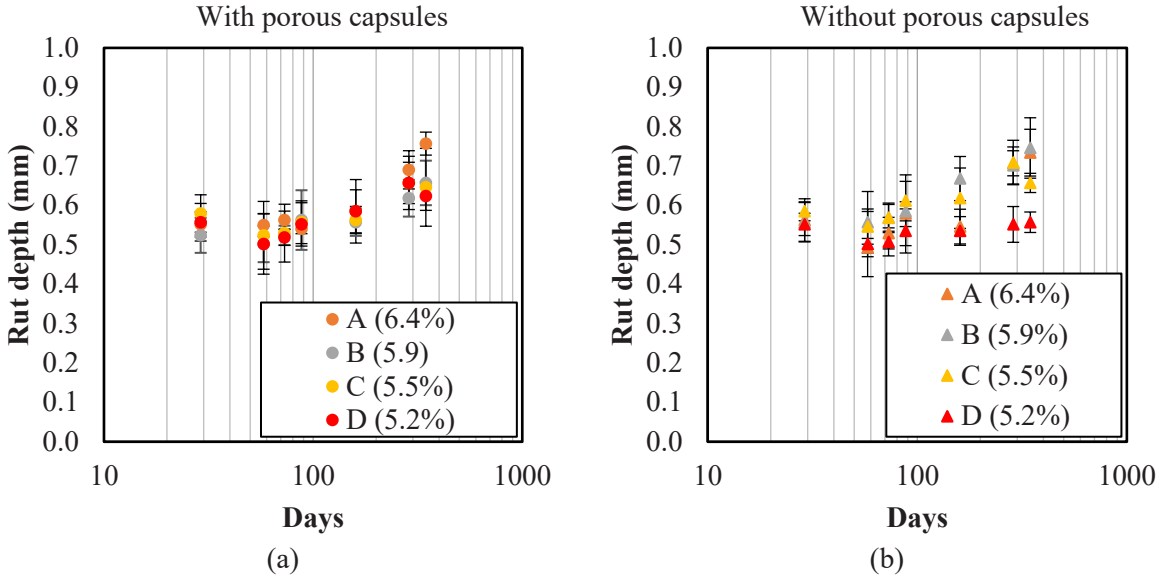

Fig. 17. Rutting evolution for each section with and without capsules.

ageing, the void content was lowered because of traffic and dust-filled voids

2. The stiffness ageing factor before road ageing is 15 %-20 % lower for asphalt with lower binder content, C and D and with capsules. After ageing, the stiffness increases in all materials; however, with capsules, it is statistically lower than that of the controlled material due to the (i) release of oil softening the binder, (ii) deformation of the capsules and further energy absorption and redistribution of the loads by providing a better skeleton performance.
3. Unaged and aged asphalt with porous capsules have higher mass loss resistance than without capsules. The higher the binder content, the higher the difference. Before site ageing, aggregate percentage loss in materials with capsules and higher binder content ranges between 25 % and 30 % and with lower binder content between 24 % and 15 %.
4. Fatigue life for unaged and aged asphalt with capsules is similar to the reference mixture. The difference in stiffness decay ratio measured under the load control test suggests a more deformable material.
5. Macrotexture evolution, along with rutting, shows a similar trend with and without capsules, indicating common asphalt behaviour in the initial days after compaction. The migration happens when bitumen is pushed to the surface; after wearing off, the macrotexture is increased to a stable level until the macrotexture is higher than the dust size, where stripping can begin. Adding capsules enhances load distribution, slowing bitumen migration and delaying aggregate erosion.

Building upon the findings of this study, future research might continue investigating the magnitude of the benefit of using asphalt with oil-filled porous capsules by continuously monitoring the trial site, along with a carbon footprint assessment, to provide a life cycle assessment and a cost estimate of using capsules with sunflower oil or other rejuvenator alternatives, e.g. recycled vegetable oil [70], that could be more

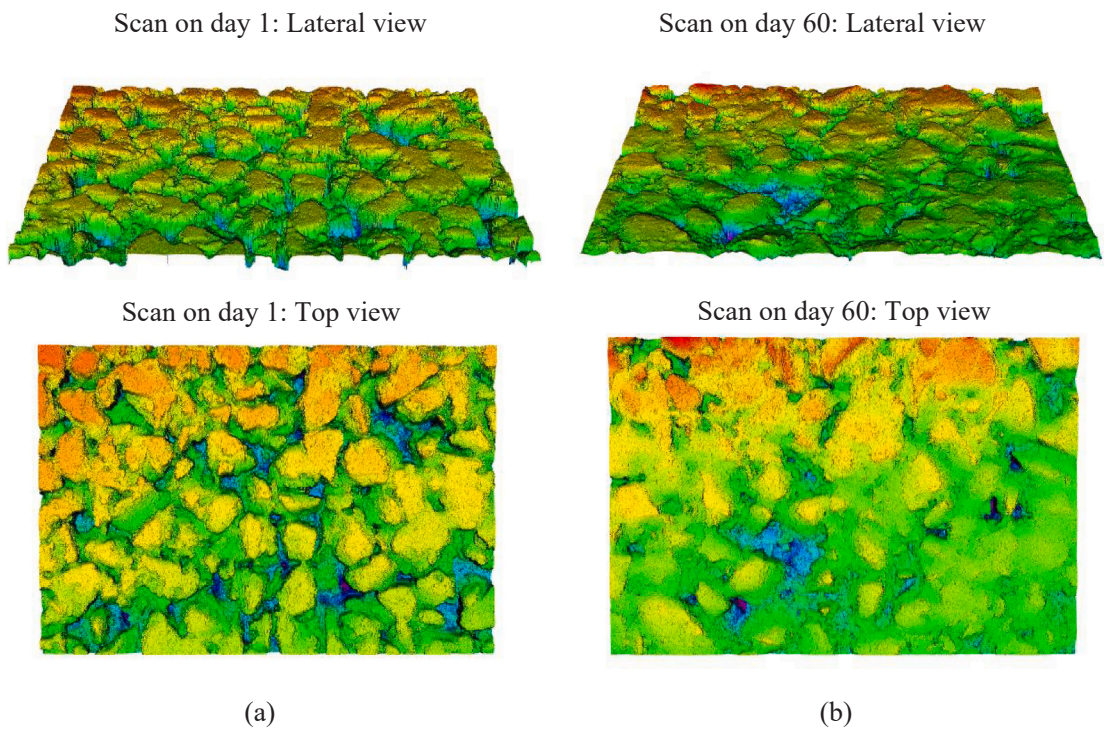

Fig. 18. 3D re-constructed scan from scanned lines in the same location on day 1 and after 60 days.

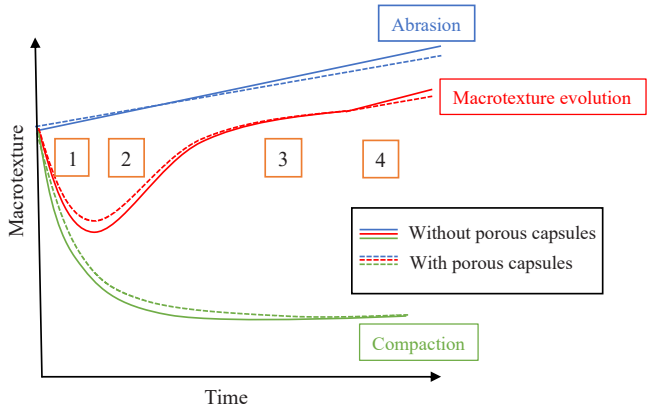

Fig. 19. Schematic explanation of macrotexture evolution with and without porous capsules.

affordable.

CRediT authorship contribution statement

Lingling Li: Writing – review & editing. **Frank Haughey:** Supervision, Project administration, Funding acquisition. **Nick Thom:** Writing – review & editing, Supervision. **Mariam Abedraba-Abdalla:** Writing – review & editing, Writing – original draft, Methodology, Investigation, Formal analysis, Data curation, Conceptualization. **A. Garcia-Hernández:** Writing – review & editing, Supervision, Project administration, Conceptualization.

Declaration of Competing Interest

The authors declare the following financial interests/personal relationships which may be considered as potential competing interests. Mariam Abedraba-Abdalla reports financial support and administrative support were provided by the University of Nottingham & Tarmac

Data availability

Data will be made available on request.

Acknowledgements

This project was supported and funded by Connect Plus M25 Ltd. The authors thank Robert Murray and Frank Haughey for their help during the project. The authors would also like to thank the Nottingham Transportation Engineering Center staff for their assistance and support during the upscaling of the equipment.

References

[1] F.M. Nejad, E. Aflaki, M.A. Mohammadi, Fatigue behavior of SMA and HMA mixtures, Constr. Build. Mater. vol. 24 (7) (Jul. 2010) 1158–1165, https://doi.org/10.1016/J.CONBUILDMAT.2009.12.025.
[2] P. Kumar, S. Chandra, S. Bose, Laboratory investigations on SMA mixes with different additives, Int. J. Pavement Eng. vol. 8 (1) (Mar. 2007) 11–18, https://doi.org/10.1080/10298430600987381.
[3] N. Ramzanpour, A. Mokhtari, Laboratory evaluation of SMA mixtures containing different additives, J. Appl. Sci. vol. 11 (22) (2011) 3677–3687, https://doi.org/10.3923/JAS.2011.3677.3687.
[4] S. Serin, N. Morova, M. Saltan, S. Terzi, Investigation of usability of steel fibers in asphalt concrete mixtures, Constr. Build. Mater. vol. 36 (Nov. 2012) 238–244, https://doi.org/10.1016/J.CONBUILDMAT.2012.04.113.
[5] M. Mohammed, T. Parry, N. Thom, J. Grenfell, Microstructure and mechanical properties of fibre reinforced asphalt mixtures, Constr. Build. Mater. vol. 240 (Apr. 2020), https://doi.org/10.1016/j.conbuildmat.2019.117932.
[6] C. Achilleos, D. Hadjimitsis, K. Neocleous, K. Pilakoutas, P.O. Neophytou, S. Kallis, Proportioning of steel fibre reinforced concrete mixes for pavement construction and their impact on environment and cost, Sustainability vol. 3 (7) (2011) 965–983, https://doi.org/10.3390/su3070965.
[7] H.U. Bahia and R. Davies, "Effect of Crumb Rubber Modifiers (CRM) on Performance-Related Properties of Asphalt Binders".
[8] J. Zhu, B. Birgisson, N. Kringos, Polymer modification of bitumen: advances and challenges, Eur. Polym. J. vol. 54 (1) (May 2014) 18–38, https://doi.org/10.1016/J.EURPOLYMJ.2014.02.005.
[9] A. Riekstins, V. Haritonovs, V. Straupe, Economic and environmental analysis of crumb rubber modified asphalt, Constr. Build. Mater. vol. 335 (Jun. 2022) 127468, https://doi.org/10.1016/J.CONBUILDMAT.2022.127468.

[10] D. Sun, B. Li, F. Ye, X. Zhu, T. Lu, Y. Tian, Fatigue behavior of microcapsule-induced self-healing asphalt concrete, J. Clean. Prod. vol. 188 (Jul. 2018) 466–476, https://doi.org/10.1016/J.JCLEPRO.2018.03.281.
[11] T. Al-Mansoori, R. Micaelo, I. Artamendi, J. Norambuena-Contreras, A. Garcia, Microcapsules for self-healing of asphalt mixture without compromising mechanical performance, Constr. Build. Mater. vol. 155 (Nov. 2017) 1091–1100, https://doi.org/10.1016/J.CONBUILDMAT.2017.08.137.
[12] N. Ruiz-Riancho, T. Saadoon, A. Garcia, R. Hudson-Griffiths, Enhanced self-healing properties in stone mastic asphalt with encapsulated bitumen rejuvenators, RILEM Book. vol. 27 (2022) 711–717, https://doi.org/10.1007/978-3-030-46455-4_90/COVER.
[13] J. Norambuena-Contreras, E. Yalcin, R. Hudson-Griffiths, A. García, Mechanical and self-healing properties of stone mastic asphalt containing encapsulated rejuvenators, J. Mater. Civ. Eng. vol. 31 (5) (May 2019), https://doi.org/10.1061/(ASCE)MT.1943-5533.0002687.
[14] L. Traseira-Piñeiro, M. Bodaghi, A. Grizi, A. Garcia-Hernandez, G. Albertini, Energy-absorbing particles for enhanced mechanical performance of asphalt's aggregate skeleton, Constr. Build. Mater. vol. 415 (Feb. 2024) 135055, https://doi.org/10.1016/j.conbuildmat.2024.135055.
[15] J. Norambuena-Contreras, E. Yalcin, A. Garcia, T. Al-Mansoori, M. Yilmaz, R. Hudson-Griffiths, Effect of mixing and ageing on the mechanical and self-healing properties of asphalt mixtures containing polymeric capsules, Constr. Build. Mater. vol. 175 (Jun. 2018) 254–266, https://doi.org/10.1016/J.CONBUILDMAT.2018.04.153.
[16] Y. He, K. Xiong, J. Zhang, F. Guo, Y. Li, Q. Hu, A state-of-the-art review and prospectives on the self-healing repair technology for asphalt materials, Constr. Build. Mater. vol. 421 (Mar. 2024) 135660, https://doi.org/10.1016/J.CONBUILDMAT.2024.135660.
[17] I. Gonzalez-Torre, J. Norambuena-Contreras, Recent advances on self-healing of bituminous materials by the action of encapsulated rejuvenators, Constr. Build. Mater. vol. 258 (Oct. 2020) 119568, https://doi.org/10.1016/J.CONBUILDMAT.2020.119568.
[18] R. Micaelo, A.C. Freire, G. Pereira, Asphalt self-healing with encapsulated rejuvenators: effect of calcium-alginate capsules on stiffness, fatigue and rutting properties, Mater. Struct. /Mater. Et. Constr. vol. 53 (1) (Feb. 2020) 1–17, https://doi.org/10.1617/S11527-020-1453-7/FIGURES/10.
[19] L. Traseira-Piñeiro, M. Bodaghi, A. Grizi, A. Garcia-Hernandez, G. Albertini, Energy-absorbing particles for enhanced mechanical performance of asphalt's aggregate skeleton, Constr. Build. Mater. vol. 415 (Feb. 2024) 135055, https://doi.org/10.1016/J.CONBUILDMAT.2024.135055.
[20] S. Pérez-Tamarit, E. Solórzano, A. Hilger, I. Manke, M.A. Rodríguez-Pérez, Multi-scale tomographic analysis of polymeric foams: a detailed study of the cellular structure, Eur. Polym. J. vol. 109 (Dec. 2018) 169–178, https://doi.org/10.1016/J.EURPOLYMJ.2018.09.047.
[21] L. Traseira-Piñeiro, T. Parry, F. Haughey, A. Garcia-Hernandez, Performance of plant-produced asphalt containing cellular capsules, Materials vol. 15 (23) (Dec. 2022), https://doi.org/10.3390/ma15238404.
[22] A. Garcia, J. Norambuena, R. Micaelo, and T. Al Mansouri, "Capsules for asphalt self-healing," Chennai, 2017.
[23] R. Micaelo, A.C. Freire, G. Pereira, Asphalt self-healing with encapsulated rejuvenators: effect of calcium-alginate capsules on stiffness, fatigue and rutting properties, Mater. Struct. /Mater. Et. Constr. vol. 53 (1) (Feb. 2020), https://doi.org/10.1617/s11527-020-1453-7.
[24] J. Norambuena-Contreras, Q. Liu, L. Zhang, S. Wu, E. Yalcin, A. Garcia, Influence of encapsulated sunflower oil on the mechanical and self-healing properties of dense-graded asphalt mixtures, Mater. Struct. /Mater. Et. Constr. vol. 52 (4) (Aug. 2019) 1–13, https://doi.org/10.1617/S11527-019-1376-3/TABLES/3.
[25] N. Ruiz-Riancho, T. Saadoon, A. Garcia, D. Grossegger, R. Hudson-Griffiths, Optimisation of self-healing properties for asphalts containing encapsulated oil to mitigate reflective cracking and maximize skid and rutting resistance, Constr. Build. Mater. vol. 300 (Sep. 2021) 123879, https://doi.org/10.1016/J.CONBUILDMAT.2021.123879.
[26] T. Al-Mansoori, J. Norambuena-Contreras, R. Micaelo, A. Garcia, Self-healing of asphalt mastic by the action of polymeric capsules containing rejuvenators, Constr. Build. Mater. vol. 161 (Feb. 2018) 330–339, https://doi.org/10.1016/J.CONBUILDMAT.2017.11.125.
[27] Á. García, E. Schlangen, M. van de Ven, G. Sierra-Beltrán, Preparation of capsules containing rejuvenators for their use in asphalt concrete, J. Hazard Mater. vol. 184 (1–3) (2010) 603–611, https://doi.org/10.1016/J.JHAZMAT.2010.08.078.
[28] "BS EN 13108–5; Bituminous Mixtures. Material Specifications. Stone Mastic Asphalt. British Standards Institution.," London, UK, 2016.
[29] N. Ruiz-Riancho, A. Garcia, D. Grossegger, T. Saadoon, R. Hudson-Griffiths, Properties of Ca-alginate capsules to maximise asphalt self-healing properties, Constr. Build. Mater. vol. 284 (May 2021) 122728, https://doi.org/10.1016/J.CONBUILDMAT.2021.122728.
[30] V. Grubelnik, M. Marhl, Drop formation in a falling stream of liquid, Am. J. Phys. vol. 73 (5) (May 2005) 415–419, https://doi.org/10.1119/1.1866100.
[31] A.M. Donald, The use of environmental scanning electron microscopy for imaging wet and insulating materials, Nat. Mater. 2003 2:8 vol. 2 (8) (2003) 511–516, https://doi.org/10.1038/nmat898.
[32] D.J. Stokes, Recent advances in electron imaging, image interpretation and applications: environmental scanning electron microscopy, Philos. Trans. R. Soc. Lond. Ser. A: Math., Phys. Eng. Sci. vol. 361 (1813) (Dec. 2003) 2771–2787, https://doi.org/10.1098/RSTA.2003.1279.
[33] T.F. Fwa, L. Chu, The concept of pavement skid resistance state, Road. Mater. Pavement Des. vol. 22 (1) (2021) 101–120, https://doi.org/10.1080/14680629.2019.1618366.
[34] "BS EN 13036–4:2003 Road and airfield surface characteristics. Test methods. Method for measurement of slip/skid resistance of a surface. The pendulum test," London, UK, 2003.
[35] "BS ISO 13473–2:2002 Characterization of pavement texture by use of surface profiles. Terminology and basic requirements related to pavement texture profile analysis.," 2002.
[36] "BS EN ISO 13473–1; Characterization of Pavement Texture by Use of Surface Profiles. Determination of Mean Profile Depth. British Standards Institution," London, UK, 2009.
[37] M.R. Islam, M.I. Hossain, R.A. Tarefder, A study of asphalt aging using Indirect Tensile Strength test, Constr. Build. Mater. vol. 95 (Oct. 2015) 218–223, https://doi.org/10.1016/J.CONBUILDMAT.2015.07.159.
[38] "BS EN 12697–26:2018 - TC Tracked Changes. Bituminous mixtures. Test methods. Stiffness," London, UK, 2020.
[39] A. Abouelsaad, G. White, Review of Asphalt Mixture Ravelling Mechanisms, Causes and Testing, Springer, 2022, https://doi.org/10.1007/s42947-021-00100-7.
[40] "BS EN 12697–24:2018 - TC Tracked Changes. Bituminous mixtures. Test methods. Resistance to fatigue," London, UK, 2012.
[41] S. Lv, Z. Wang, X. Zhu, J. Yuan, X. Peng, Research on strength and fatigue properties of asphalt mixture with different gradation curves, Constr. Build. Mater. vol. 364 (Jan. 2023) 129872, https://doi.org/10.1016/J.CONBUILDMAT.2022.129872.
[42] A. Garcia-Hernández, S. Salih, I. Ruiz-Riancho, J. Norambuena-Contreras, R. Hudson-Griffiths, B. Gomez-Meijide, Self-healing of reflective cracks in asphalt mixtures by the action of encapsulated agents, Constr. Build. Mater. vol. 252 (Aug. 2020) 118929, https://doi.org/10.1016/J.CONBUILDMAT.2020.118929.
[43] O. Al-Ketan, R. Rowshan, A.H. Alami, Biomimetic materials for engineering applications, Encycl. Smart Mater. (Jan. 2022) 25–34, https://doi.org/10.1016/B978-0-12-815732-9.00019-X.
[44] L. Gibson, M.F. Ashby. Cellular Solids, Second ed, Cambridge University Press, 1997.
[45] T.A. Schaedler and W.B. Carter, "Architected Cellular Materials," 2016, doi: 10.1146/annurev-matsci-070115-031624.
[46] R.A. Tarefder, M. Ahmad, Effect of compaction procedure on air void structure of asphalt concrete, Measurement vol. 90 (Aug. 2016) 151–157, https://doi.org/10.1016/J.MEASUREMENT.2016.04.054.
[47] H. Wang, et al., Effects of field aging on material properties and rutting performance of asphalt pavement, Materials vol. 16 (1) (Jan. 2023), https://doi.org/10.3390/MA16010225.
[48] N.R. Sefidmazgi, P. Teymourpour, H.U. Bahia, Effect of particle mobility on aggregate structure formation in asphalt mixtures, Road. Mater. Pavement Des. vol. 14 (S2) (2013) 16–34, https://doi.org/10.1080/14680629.2013.812844.
[49] J. Li, P. Li, J. Su, L. Yang, X. Wu, Coarse aggregate movements during compaction and their relation with the densification properties of asphalt mixture, Int. J. Pavement Eng. vol. 22 (8) (2021) 1052–1063, https://doi.org/10.1080/10298436.2019.1659263.
[50] Z.A. Khan, H.I. Al-Abdul Wahab, I. Asi, R. Ramadhan, Comparative study of asphalt concrete laboratory compaction methods to simulate field compaction, Constr. Build. Mater. vol. 12 (6–7) (Sep. 1998) 373–384, https://doi.org/10.1016/S0950-0618(98)00015-4.
[51] A.E. Alvarez, A.E. Martin, C. Estakhri, Effects of densification on permeable friction course mixtures, J. Test. Eval. vol. 37 (1) (Jan. 2009) 11–20, https://doi.org/10.1520/JTE101808.
[52] S. Sreedhar, E. Coleri, Effects of binder content, density, gradation, and polymer modification on cracking and rutting resistance of asphalt mixtures used in oregon, J. Mater. Civ. Eng. vol. 30 (11) (Nov. 2018) 04018298, https://doi.org/10.1061/(ASCE)MT.1943-5533.0002506/ASSET/E0F1BE5D-820A-4EBE-9E88-FB05DA1E3B31/ASSETS/IMAGES/LARGE/FIGURE7.JPG.
[53] H. Zhang, K. Anupam, T. Skarpas, C. Kasbergen, S. Erkens, Understanding the stiffness of porous asphalt mixture through micromechanics, Transp. Res Rec. vol. 2675 (8) (Mar. 2021) 528–537, https://doi.org/10.1177/0361198121999060/ASSET/IMAGES/LARGE/10.1177_0361198121999060-FIG10.JPEG.
[54] R. Micaelo, A.C. Freire, G. Pereira, Asphalt self-healing with encapsulated rejuvenators: effect of calcium-alginate capsules on stiffness, fatigue and rutting properties, Mater. Struct. /Mater. Et. Constr. vol. 53 (1) (Feb. 2020) 1–17, https://doi.org/10.1617/S11527-020-1453-7/FIGURES/10.
[55] S. Sreedhar, E. Coleri, The effect of long-term aging on fatigue cracking resistance of asphalt mixtures, Int. J. Pavement Eng. vol. 23 (2) (2022) 308–320, https://doi.org/10.1080/10298436.2020.1745206.
[56] "A review of asphalt and asphalt mixture aging: Una revisión." Accessed: Apr. 02, 2024. [Online]. Available: http://www.scielo.org.co/scielo.php?pid=S0120–56092013000100002&script=sci_arttext
[57] C. Shi, et al., Research on the evolution of aggregate skeleton characteristics of asphalt mixture under uniaxial compression loading, Constr. Build. Mater. vol. 413 (Jan. 2024) 134769, https://doi.org/10.1016/J.CONBUILDMAT.2023.134769.
[58] S. Wang, W. Yu, Y. Miao, L. Wang, Review on load transfer mechanisms of asphalt mixture meso-structure, Materials vol. 16 (3) (Feb. 2023) 1280, https://doi.org/10.3390/MA16031280.
[59] X. Wang, J. Ren, X. Gu, N. Li, Z. Tian, H. Chen, Investigation of the adhesive and cohesive properties of asphalt, mastic, and mortar in porous asphalt mixtures, Constr. Build. Mater. vol. 276 (Mar. 2021) 122255, https://doi.org/10.1016/J.CONBUILDMAT.2021.122255.

[60] M. Guo, X. Yin, X. Du, Y. Tan, Effect of aging, testing temperature and relative humidity on adhesion between asphalt binder and mineral aggregate, Constr. Build. Mater. vol. 363 (Jan. 2023) 129775, https://doi.org/10.1016/J.CONBUILDMAT.2022.129775.
[61] A. Chen, G. Liu, Y. Zhao, J. Li, Y. Pan, J. Zhou, Research on the aging and rejuvenation mechanisms of asphalt using atomic force microscopy, Constr. Build. Mater. vol. 167 (Apr. 2018) 177–184, https://doi.org/10.1016/J.CONBUILDMAT.2018.02.008.
[62] M. Guo, M. Liang, A. Sreeram, A. Bhasin, D. Luo, Characterisation of rejuvenation of various modified asphalt binders based on simplified chromatographic techniques, Int. J. Pavement Eng. vol. 23 (12) (Oct. 2022) 4333–4343, https://doi.org/10.1080/10298436.2021.1943743.
[63] L. Traseira Piñeiro, T. Parry, F. Haughey, A. Garcia-Hernández, Architected cellular particles to mitigate asphalt stone loss, Constr. Build. Mater. vol. 328 (Apr. 2022) 127056, https://doi.org/10.1016/J.CONBUILDMAT.2022.127056.
[64] Bituminous mixtures. Test method Specimen prepared by roller compactor, "BS EN 12697–33:2019," p. 19, Accessed: Sep. 26, 2022. [Online]. Available: https://www.en-standard.eu/bs-en-12697–33-2019-bituminous-mixtures-test-method-specimen-prepared-by-roller-compactor/
[65] H. Ziari, A. Amini, A. Goli, The effect of different aging conditions and strain levels on relationship between fatigue life of asphalt binders and mixtures, Constr. Build. Mater. vol. 244 (May 2020) 118345, https://doi.org/10.1016/J.CONBUILDMAT.2020.118345.
[66] P.K. Meena, G. Saha, K.P. Biligiri, Estimation of fatigue life using resilient moduli of asphalt mixtures, J. Test. Eval. vol. 44 (1) (Jan. 2016) 424–438, https://doi.org/10.1520/JTE20140373.
[67] D.J. Wilson, R. Charles, and M. Dunn, "Polishing aggregates to equilibrium skid resistance," 2005. [Online]. Available: https://www.researchgate.net/publication/228564503.
[68] "ASTM E303 Standard Test Method for Measuring Surface Frictional Properties Using the British Pendulum Tester." Accessed: Apr. 15, 2024. [Online]. Available: https://www.astm.org/e0303–22.html
[69] Y. Tsai and Z. Wang, "Development of an Asphalt Pavement Raveling Detection Algorithm Using Emerging 3D Laser Technology and Macrotexture Analysis Final Report for NCHRP IDEA Project 163," 2015, Accessed: Apr. 18, 2024. [Online]. Available: www.trb.org/idea.
[70] I.N. Usanga, F.O. Okafor, C.C. Ikeagwuani, Effect of recycled vegetable oil on the performance of nanomarl-modified asphalt mixtures, J. Infrastruct. Preserv. Resil. vol. 4 (1) (Dec. 2023) 1–18, https://doi.org/10.1186/S43065-023-00089-2/TABLES/9.